Anti-pancreatic Cancer Effects of Novel Artemisinin-containing Nanogels

by
Team TRANSPORT

Mukti Trivedi, Elisa Pierpaoli, Noam Fox, Warren Stewart, Kayla Guralnik, Elizabeth Barski, Natasha Oberoi, and Delyar Delavari

Thesis Directed By: Dr. Tao Lowe, Fischell Department of Bioengineering

This thesis is submitted to the Gemstone Faculty of the
University of Maryland, College Park, in partial fulfillment
of the requirements for the honors citation of the Gemstone Honors Program, 2024

Abstract

Pancreatic cancer has a 12% five-year survival rate in the United States, making it the fourth deadliest cancer. Current treatment options include chemotherapy with and without radiation therapy, targeted therapy, or surgery; however, these options have limited success due to low efficiency and adverse effects. In this research, we investigate the efficiency of a proprietary technology NanoART631 (PCT/US2023/019974) invented by our advisor Dr. Tao Lowe and her collaborator Dr. Curt Civin in treating pancreatic cancer. NanoART631 is a nanogel system composed of thermoresponsive poly (N-isopropylacrylamide) and biodegradable dextran-lactate-2-hydroxyethyl-methacrylate, encapsulated with an artemisinin (ART) dimer with a molecular weight of 631 Da. NanoART631 previously demonstrated effective killing of human leukemia cells and sustained the release of ART631 for more than one month in the Lowe lab. However, NanoART631 has not been tested in regard to pancreatic cancer. In our study, we used Fourier transform infrared spectra (FTIR) to characterize the chemical structures of NanoART631s containing different amounts of ART631: 0, 2, 5 and 10 wt%. We also used Zetasizer Ultra to characterize the hydrodynamic particle size, polydispersity index (PDI) and zeta-potential of NanoART631s in water and two culture media for human pancreatic PANC-1 and MiaPaCa2 cells. The results showed that NanoART631s were monodisperse with hydrodynamic diameters between 100 and 230 nm and PDI <0.25 at 37 ºC and both the cell culture media decreased the particle size and there was no difference of the effects of the two cell culture media on the particle size. The magnitudes of the zeta potential of 0, 2, 5 and 10 wt% NanoART631 in water at both room and body temperature were consistently below 20 mV. In both cell mediums at body temperature, the magnitudes of the zeta potential of 0, 2, 5 and 10 wt% NanoART631 were consistently below 5mV.

We additionally used MTT assay to study the cytotoxicity of NanoART631s to PANC-1 and MiaPaCa2 cells as a function of concentration and determined the effectiveness of NanoART631s in killing the two cells by calculating their IC_{50}s. The IC_{50}s of NanoART631s containing 2, 5 and 10 wt% ART631 were between 20 and 200 nM depending on the cell type. The effectiveness of killing the both human pancreatic cancer cells increased with increasing the amount of ART631 in the nanoparticles. The NanoART631s have potential as an effective novel therapy to treat pancreatic as well as many other cancers.

Keywords: pancreatic cancer, nanogels, artemisinin, FTIR, hydrodynamic size, polydispersity index (PDI), zeta-potential, MTT assay, cell viability, and IC_{50}

Acknowledgments

We would like to thank our mentor, Dr. Tao Lowe, for her support and guidance throughout our entire research process, from developing our cutting-edge thesis ideas to experimental designs to results analysis to thesis production and defense. We would also like to extend thanks to members of the Lowe Lab, Noha Ghonim, Sangyoon Kim, and Eman Mirdamadi for their help. We are beyond grateful to the Gemstone program for their support during the past four years and for giving us the opportunity to engage in novel research. Thank you to our discussants, Dr. Feyruz Rassool, Dr. Hem Shukla, Dr. Gregg Duncan, Dr. Matthew Katz, and Dr. Won Jin Ho, for their time and feedback, and our team librarian, Ms. Nevenka Zdravkovska. Lastly, we'd love to thank Samat Borbiev and Emily Lin for all the help he provided throughout this process.

Contributions

Protocol development: N.F., E.P, and M.T.; Cell Maintenance: E.B., N.F., E.P., N.O., and M.T.; Cytotoxicity Experiments: all authors; Nanoparticle Characterization Experiments: E.P. and M.T.; Data Analysis: K.G., E.P., W.S., and M.T.; Funding: N.O. and M.T.; Lab Administration: M.T.; Project Administration: N.F. and K.G.; Thesis presentation: N.F., K.G., and M.T. All authors contributed to the literature review, thesis writing, and revisions.

Table of Contents

Chapter 1: Introduction

Despite accounting for 3% of all cancer cases and 7% of cancer related deaths, pancreatic cancer is the fourth deadliest form of cancer in the United States.[1,2] Although the average five-year survival rate for pancreatic cancer is approximately 12%, most cases are diagnosed at an advanced stage where the survival rate is significantly reduced to 3%.[3,4] These statistics exemplify how this cancer is in fact a silent killer often gone unnoticed. Current estimates indicate that in 2023, approximately 50,550 individuals died from pancreatic cancer in the United States.[2]

Cancer is caused by the uncontrolled proliferation of mutated cells within the body. Generally, treatment consists of one or a combination of chemotherapeutic agents that are administered to target cancer cells. The current standard of care for pancreatic cancer is chemotherapy, which is expensive and largely ineffective. Chemotherapeutic drugs work by triggering apoptosis and preventing further progression of tumor growth.[5] Unfortunately, these treatments do not discriminate which cells are targeted and frequently cause cytotoxic effects on healthy cells that result in adverse effects such as hair loss, nausea, vomiting, extreme fatigue, complicated infections, and in some cases death. Additionally, traditional chemotherapies have many limitations including low bioavailability, poor water solubility, and short half-life in the bloodstream.[2,5] One way to combat the common pitfalls of traditional chemotherapeutics is through the use of nanoparticles.

To overcome these limitations, researchers have begun utilizing nanoparticles to tailor the drugs' pharmacokinetic properties including absorption, metabolism, distribution, and elimination. Nanoparticles can also increase the penetration of drugs across biological barriers; deliver drugs to a specified target/site/cell/tissue/organ to reduce off-target effect and systemic

toxicity; and sustain the release of drugs to the targeted site to reduce frequency of administration and improve patient compliance.[6] Nanogels, a subsection of nanoparticles, have unique properties that make them adaptable for diverse conditions due to their high sensitivity to environmental conditions. Unlike nanoparticles, they have a crosslinked-polymer structure that allow the structure to shrink or expand based on environmental stimuli like pH and temperature. Often, nanogels function by retaining large amounts of water and exhibit a swelling and deswelling mechanism. These adaptable properties allow for facilitated delivery of the carried drug to the site of interest in the body as well as a controlled release of their carried drug based on specific conditions. Importantly, successful nanogels themselves are non-toxic and do not cause harmful side effects unless administered at extremely high dosages.

Artemisinin, a drug derived from sweet wormwood to treat malaria and was then synthesized into ART631 by Dr. Curt Civin's group to become more effective against cancer. Preliminary results with ART631 have demonstrated significant anticancer properties on leukemia cells with no cytotoxicity to healthy retinal endothelial cells and dental pulp stem cells.[7] ART631 has a unique endoperoxide bridge which is the main reason why it is toxic to cancer cells. One mechanism of action involves induction of ferroptosis, an oxidative, iron-dependent form of regulated cell death, which can be induced by ART631 due to its endoperoxide bridge that breaks into reactive oxygen species (ROS) when it interacts with a heme-iron group [8,9] and the fact that ferritin, a major iron storage protein, is overexpressed in cancer cells. Another main method by which ART631 can kill cancer cells is through inducing autophagy by triggering mitochondrial dysfunction because of ROS generation. Other common methods include cell cycle arrest and augmentation of apoptosis, both of which are caused by numerous specific pathways, but can also be connected to ROS production.[10]

The tumorigenicity is significantly impacted because many cancers have elevated iron concentrations compared to healthy tissue, meaning that artemisinin should be more effective at specifically targeting and inhibiting cancerous cells.[10] Dr. Curt Civin's Lab is investigating ART631 as a treatment for leukemia. The lab has found that ART631 is a strong candidate for future cancer research as it can inhibit cancerous growth at comparable rates to certain chemotherapeutics, but is non-toxic to healthy tissue. However, while having strong anticancer properties, the research indicated that ART631 has poor water solubility, a short half-life, and low bioavailability in the body. To address this issue, Dr. Tao Lowe's Lab formulated ART631 into a nanogel, called NanoART631 as shown in Scheme 1.

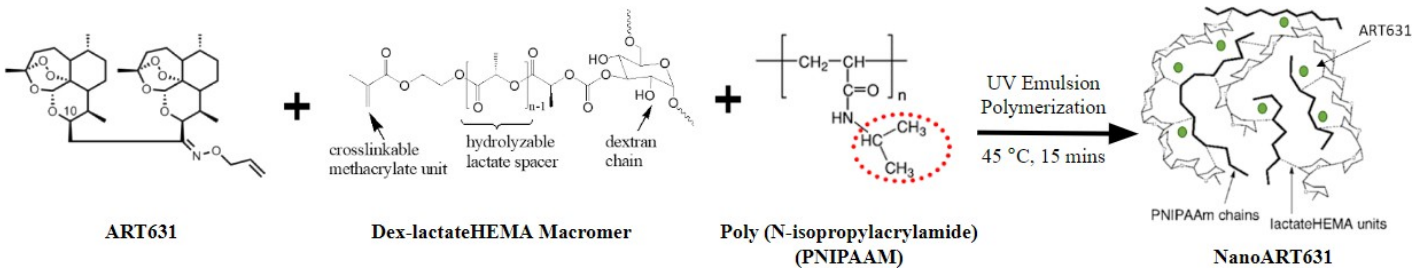

Scheme 1. Chemical structure of Artemisinin and nanogel compound.[10–12]

NanoART631 is the combination of ART631 with a unique nanogel formulation (Scheme 1). It fully encapsulates artemisinin, sequesters it, and releases it at or near cancerous tissue. Loading the nanogel with ART631 improves the effects of the drug by facilitating a site-specific and controlled release of ART631. Since NanoART631 has not been investigated on pancreatic cancer, in this study, under Dr. Lowe's mentorship, we evaluated the effectiveness of NanoART63s containing different amounts of ART631: 0, 2, 5 and 10 wt% in killing two human pancreatic cancer cell lines, PANC-1 and MIA PaCa-2, *in vitro* using MTT assay. Before the cytotoxicity study, we also used FTIR to characterize the chemical structures of NanoART631s

and used Zetasizer Ultra to measure the hydrodynamic particle size, polydispersity index (PDI) and zeta-potential of NanoART631s in water and two culture media for PANC-1 and MIA PaCa-2 cells. Our results demonstrated that NanoART631s have potential to be an effective novel nanotherapy to treat pancreatic as well as many other cancers.

Chapter 2: Literature Review

Pancreatic Cancer

Pancreas Anatomy and Function

One of the pancreas' primary purposes is to aid in the digestive process. This is governed by the exocrine gland, which secretes digestive enzymes through channels at the pancreatic duct. These enzymes, along with a bicarbonate, help break down carbohydrates, fats, proteins, and neutralize acids before they enter the duodenum, thus preventing damage to the rest of the digestive system.[13] Another primary function of the pancreas is to secrete vital hormones into the bloodstream via the endocrine gland. The pancreas produces insulin and glucagon, which regulates the level of glucose in the blood. Additionally, somatostatin, also released by the endocrine gland, manages the amount of insulin and glucagon being released by the pancreas.[13] If these processes are interrupted, there can be dire consequences. When the pancreas is nonfunctional, the body cannot absorb nutrients in food, leading to painful side effects such as malnutrition, diarrhea, weight loss, bone pain from a Vitamin D deficiency, or excessive bleeding from a Vitamin K deficiency.[13]

Cancer In General

While originating from a single cell, a culmination of genetic mutations leads to a fatal prognosis for thousands of patients every year. This single cell will then continue to grow and invade surrounding tissues or spread to other parts of the body, often disrupting critical functions within the body which may lead to death. Unlike pathogens that invade and feed off the resources of the host, cancer cells originate from healthy cells that have undergone multiple genetic mutations. Some mutations are caused by environmental factors like radiation, lifestyle, or diet, while others are caused by errors during cellular replication. These mutations begin to

aggregate which can result in replicative immortality and resistance to cell death. Finally, as the tumor grows, it will begin angiogenesis to provide additional blood flow to continue supplying nutrients to itself as well as activating metastasis, which heavily lowers prognosis.[14]

Pancreatic Cancer

Pancreatic cancer is the fourth leading cause of cancer related death in both men and women. It has a poor prognosis, with over 80% of patients exhibiting regional spread or metastatic disease at the point of diagnosis. The pancreas has three main areas: the head, the body, and the tail, with the tail being more prone to metastases.[15] Risk factors of pancreatic cancer include smoking, diabetes mellitus, and BRCA2 gene mutations. Additionally, it is more prevalent in African American and male communities compared to the broader population. However, the primary risk assessment tool for pancreatic cancer is family history.

Symptoms may present as common side effects of other diseases, such as the stomach flu.[15] Patients report experiencing dull, nonspecific pain, which normally results from the tumor spreading to the celiac and superior mesenteric arterial plexus located behind the stomach. They may also experience nausea, anorexia, weight loss, and sudden onset diabetes resulting from the weakening of the pancreas' endocrine gland.[15]

More than 90% of pancreatic cancer diagnoses are for pancreatic adenocarcinoma, which originates from the exocrine ducts of the pancreas. Adenocarcinoma can also develop from the cells that secrete, synthesize, and store digestive enzymes in the pancreas— this is known as acinar cell carcinoma and occurs in 1-2% of exocrine cancers. Squamous cell carcinoma is extremely rare, as it forms in pancreatic ducts but comprises squamous cells, which are not normally seen in the pancreas. Most of these cases are discovered after metastasis and its mechanism is not fully understood due to its rarity. Adenosquamous carcinoma occurs in 1-4%

of exocrine pancreatic cancers. This is the most aggressive tumor type, with a poorer prognosis when compared to adenocarcinoma. Colloid carcinoma occurs in 1-3% of exocrine pancreatic cancers and develops from intraductal papillary mucinous neoplasm (IPMN), which is a type of benign cyst. This is easier to treat and has a better prognosis than other pancreatic cancers because it manifests as malignant cells floating in a gelatinous substance known as mucin, which is far less likely to spread.[15,16]

The Role of Iron in Cancer

Since the drug formulation used in this study interacts with intracellular iron, it is important to discuss how iron is used as a target for cancer therapy. Iron is required to carry out the normal functions of proteins and enzymes because proteins that contain iron are necessary for cell respiration, oxygen transport, oxygen metabolism, and signaling.[17] Many types of cancers have elevated iron concentrations compared to healthy tissues because malignant cell require a higher levels of iron for cell survival and rapid proliferation, making this a plausible channel for cancer therapy.[18] Both iron excess and iron depletion can be used to treat cancer, depending on the functions that must be facilitated or suppressed.[17] In pancreatic cancer, there is a consistent correlation between iron levels and the likelihood of cancer development. Research indicates a positive association between the consumption of red meat and pancreatic cancer in men.[17] In humans, dietary iron is absorbed in the duodenum, which may be dangerous for people with an increased risk of pancreatic cancer, or those who already have it and wish to limit its growth. Increased iron consumption has been used in previous studies to induce sarcoma in rats. Thus the correlation between increased iron levels and cell growth suggests limiting the amount of iron digested could have a positive effect on prognosis.[17] Iron chelators have exhibited antitumor activity by limiting cancer cells' uptake of iron. However, this treatment has side effects

including, but not limited to, diarrhea, nausea, vomiting, and fatigue. Iron is also necessary for cellular death pathways. Both decreasing and increasing iron absorption can induce cancer cell death. Iron depletion disrupts cellular processes, and excess iron causes damage to DNA and the endoplasmic reticulum, inducing apoptosis. Excess iron can also trigger necroptosis, which occurs when the cell swells and the plasma membrane ruptures. Ascorbate and the ferroptosis process have both been utilized in anti-cancer treatments.[14,17]

Current Treatments for Pancreatic Cancer

Surgery

Only about 15-20% of pancreatic cancer patients are eligible for surgery. This is partly because 50% of pancreatic cancer is diagnosed in stage IV, at which point the cancer has metastasized and surgery is futile. Even with surgery, patients typically have a 20-30% five-year survival rate.[19] The primary surgical technique, the Whipple procedure, involves removing the head of the pancreas, the duodenum, and other parts of the digestive tract. This procedure can have long-term impacts on the patient's digestive health.[20] Another surgical option is the distal or total pancreatectomy, where a portion or the whole pancreas is removed along with the spleen (distal) and portions of the gallbladder, bile duct, intestines, and stomach (total). In addition to changes in digestive health, these procedures leave patients unable to produce insulin,thus making them take supplemental enzymes for the rest of their lives.[21] In terms of cost, surgery can be quite expensive, especially without insurance. On average surgery costs $40,000-50,000 and additional costs can be accrued if complications arise.[22]

Radiation

Radiation therapy is commonly used in conjunction with chemotherapy or surgery. Most commonly, radiation therapy is administered via an external beam which focuses radiation from a source outside the body on the cancerous region. The experience is quite similar to an X-ray except with significantly stronger radiation. Before surgery, radiation, in conjunction with chemotherapy, can shrink a tumor;after surgery radiation can decrease the risk of recurrence. Hence, chemoradiation therapy (chemo combined with radiation) is the choice treatment for patients with more advanced stages. In addition to hindering tumor growth, radiation can be used to ease symptoms of cancer and increase patient quality of life.[23] The cost of radiation therapy varies depending on the type, frequency, and location. Before insurance, costs can range from $9,000 to $12,000 monthly, insurance coverage varies based on plan.[24] In addition to the financial side effects, radiation can affect nearby healthy cells in addition to cancer cells, which causes detrimental symptoms for patients. Some side effects include: nausea, diarrhea, fatigue, loss of appetite, weight loss, and an increased risk of infection.[23]

Ablation

Radiofrequency ablation (RFA) is being increasingly used for unresectable solid organ tumors. This treatment involves delivering thermal energy to the tumor via electrodes resulting in necrosis and protein denaturation and ultimately decreased tumor size. Unfortunately, this treatment is palliative for advanced cases and carries a high risk of complications.[25]

Chemotherapy

Chemotherapy utilizes pharmaceutical drugs to prevent or destroy tumors. Drugs are delivered to the pancreas, typically orally or intravenously, to alter the chemical and physical composition of the cancer cells' environment or their function. Chemotherapy can be used at any stage and is often used in conjunction with surgery or radiation. Before surgery, chemotherapy

can be used to shrink a tumor to simplify surgery. Afterward, chemotherapy can treat any remaining cancerous cells that were left behind by previous treatment and minimize the risk of recurrence. Additionally, chemotherapy can be paired with radiation to bolster both treatments.[26] Chemo can be quite costly to the patient depending on which drugs are used and the frequency of dosing. For patients with Medicare, the average claim for chemo costs approximately $40,000.[27] Additionally, while chemotherapy is intended to target only cancerous cells, it could potentially have a negative impact on healthy cells and can therefore be detrimental to patients health in the long term. Common pancreatic cancer chemotherapy drugs include Gemcitabine, Paclitaxel Albumin-stabilized Nanoparticle Formulation combined with Gemcitabine, Erlotinib Hydrochloride combined with Gemcitabine, Everolimus, Fluorouracil, Irinotecan Hydrochloride Liposome, Olaparib, and Mitomycin.

Artemisinin and ART631

Artemisinin is a drug derived from the plant, *Artemisia annua* (sweet wormwood), which originally was used to treat malaria. Derivatives of the natural product have since been synthesized and proven to show significant activity against a variety of diseases and cancers.[28] Artemisinin and its derivatives are all sesquiterpene lactones (sesquiterpenes with a lactone ring). Due to its unique structure, artemisinin has been shown to not cause healthy cellular damage while still reducing tumor size. It is hypothesized that the endoperoxide bridge in this compound (R-O-O-R') is activated by reduced heme-iron groups, leading to the formation of carbon-centered free radicals.

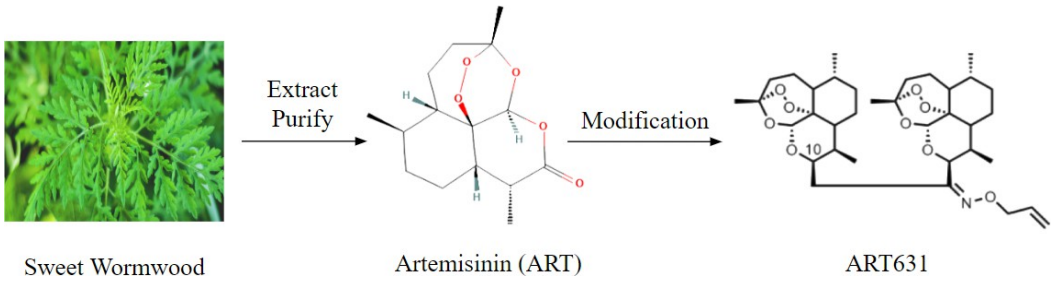

Scheme 2. Chemical structure of Artemisinin and ART631.[8]

While the mechanism of action has not been fully illustrated in literature, a current hypothesis is that the generation of free radicals from the interaction with intracellular iron causes cytotoxicity and ultimately apoptosis in cells.[9,13] Those free radicals damage susceptible proteins and cause cellular death of cancer cells because malignant cells require a higher level of iron metabolism for cell survival and rapid proliferation.[18] This mechanism causes artemisinin to be incredibly effective and potent in killing cancer cells while remaining comparatively non toxic towards healthy cells, although not entirely non toxic.[14] Hence, artemisinin is a strong candidate for future cancer research as it can inhibit cancerous growth at comparable rates to certain prescribed chemotherapeutics, but is less toxic to healthy tissue. However, artemisinin has not been extensively explored in current cancer research due to its low half-life and has only recently been introduced into oncology research as a possible avenue for cancer treatment. Additionally, like many other chemotherapy treatments, it has some cytotoxic effects on healthy cells. Due to artmisinin's effective anticancer mechanism, derivatives of the natural product have since been synthesized and proven to show significant activity against a variety of diseases and cancers.[28] ART631 is one derivative of artemisinin, developed by Dr. Curt Civin's group (Scheme 2). Preliminary results demonstrated that ART631 has significant anticancer effects for treating leukemia.[7] *In vitro* studies done by Dr. Civin's group found that ART631 had potent activity against MOLM14, an Acute Myeloid Leukemia (AML) cell line, in comparison to the

first-generation derivative artesunate. Further, ART631 was shown to inhibit growth in 9 out of 10 AML cell lines by decreasing levels of the anti-apoptotic protein MCL1.[29]

Nanoparticles and Nanogels

History of Nanoparticles

While nanoparticles and nanotechnology have been on the rise for the past decade, the idea of nanomedicine stems from as early as the 1990s.[30] The first uses of nanomaterials come from nanoporous ceramic filters separating viruses.[30] As nanotechnology developed the areas of use also evolved. The 20th century was when the first nanoparticle for drug delivery was developed by Peter Paul Speiser.[30] Nanotechnology can be used to move substances to specific areas of the body, change and modify genetic information, for diagnosis purposes, and various treatments.[30] Additionally, nanoparticles can be used for optical imaging which would focus on blood vessels, lymph nodes, and specific tumor sites.[31] Furthermore, magnetic resonance imaging, also known as MRI, can utilize nanotechnology for cancer detection.[31]

Nanoparticles were introduced by Nobel laureate Richard Feynman in 1960 but began to gain traction in the medical field in the early 1990s.[30,32] Major challenges associated with treating cancer include the early detection of the disease and harmful side effects associated with treatment. [33] Nanoparticles provide a solution for these challenges because they can be engineered to penetrate many biological barriers in the body to reach their targeted site. This greatly reduces the side effects that people can experience when doing chemotherapy treatment, which are generally caused by the highly toxic medicine attacking healthy cells as well as cancerous cells.

Nanoparticles and Their Properties

Nanoparticles (NPs) are a broad class of materials defined as particles between 1 and 100 nm in size.[32] Their small size and unique chemical properties can improve the solubility of certain drugs, bypass barriers within the body, and lessen side effects.[31] Nanoparticles have been implemented in a variety of ways, including cancer therapy, vaccinations, contraceptives, diagnosis, biosensing and bioimaging devices, tissue engineering, etc.[31]

Since cancer is the second leading cause of death in the United States, significant research surrounding nanoparticles' ability to transport various drugs to targeted areas while avoiding any damage to healthy tissue continues to be investigated. The incorporation of nanoparticles greatly reduces the side effects that people experience when undergoing chemotherapy, which are usually caused by the highly toxic medicine attacking healthy cells.

The size of the nanoparticle is integral in determining its properties. An advantage of nanoparticles is their ability to enter the cell. Nanoparticles are taken up by cells via endocytosis, and depending on the specific mechanism, cells can internalize nanoparticles ranging from 40 to over 200 nm.[34] Due to the nature of these mechanisms, cells can more easily integrate smaller molecules (ranging around 100 nm). On the other hand, smaller nanoparticles release drugs at a faster rate but also aggregate more readily, potentially causing increased side effects.[35] An example of how nanoparticle size affects the toxicity of a formulation, Huo et al. demonstrated that gold NPs no larger than 6 nm effectively enter the cell nucleus, whereas large NPs (10 or 16 nm) only penetrate through the cell membrane and are found only in the cytoplasm.[36] This indicates that smaller NPs are more toxic than larger NPs, which cannot enter the nucleus (when not taking shape and surface charge of these nanoparticles into consideration).[37]

Relating to cancer therapy, many scientists take advantage of the enhanced permeability and retention (EPR) effect of cancer. The EPR effect allows nanoparticles to passively accumulate at tumor sites due to leaky blood vessels and pores (which are characteristic of cancer) that allow particles over 100 nm big to pass through and accumulate near the cells.[38] This would not be possible with healthy blood vessels. Along with particle size, the shape of NPs affects their ability to move throughout the human body and through various barriers such as the blood-brain barrier.[39] Rod-shaped particles can enter cells quickly, up to four times the speed of shorter, more cylindrical-shaped particles. Synthesizing particles of more complex shapes has been challenging, but research indicates that the shape makes a significant difference in the human body's response to a given drug.[40]

A positive surface charge has been found to correlate with higher cellular uptake and cytotoxicity in phagocytic cells, which is key for eliminating cancer cells. However, NPs with a negative surface charge appear to have the same effect on nonphagocytic cells. The kind of cell being targeted must be taken into account when designing a nanoparticle for a specific condition, as it would be prudent to avoid unnecessary side effects on the patient as a result of more inefficient uptake.[41]

Nanogels

Nanogels are composed of three-dimensional crosslinked hydrogel materials in the nanoparticle size range that are formed by physically or chemically cross-linking water-soluble polymers to create a swellable, insoluble polymer network.[9,42] They can be composed of naturally occurring polymers, synthetic polymers, or a combination of the two (Scheme 3).

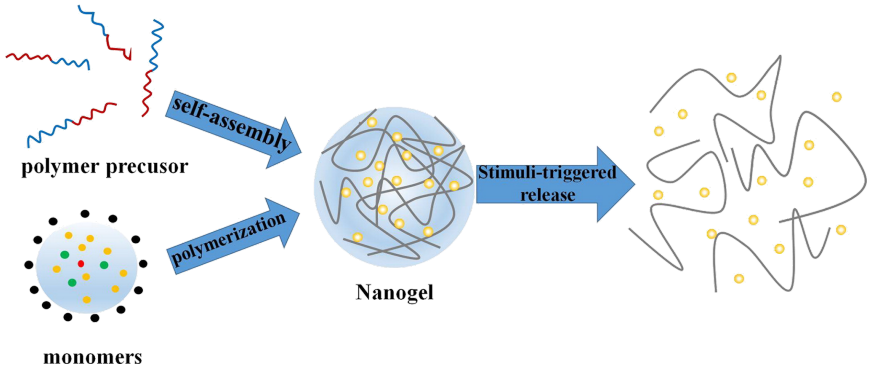

Scheme 3. Illustration of nanogel synthesis and drug release.[42]

Due to their composition, nanogels can effectively combine the properties of hydrogels and nanoparticles. Like nanoparticles, they can improve drug solubility, increase the stability of drugs, increase site-specific drug accumulation, and lower the cytotoxic effects of certain drugs. Their hydrogel component allows them to possess a high capacity to hold water without dissolving in aqueous environments like the human body. Gels are soft materials that combine the properties of solids and liquids, thus enabling nanogels' high bioavailability. Their high loading capacity, and controlled release abilities stem from their porosity and swelling capability. Thus, nanogels have excellent stability in the body, high drug-loading capacity, and the ability to respond to a variety of environmental stimuli.[42]

Nanogels have a versatile architecture, allowing variations in chemical structure to fine-tune the size, charge, porosity, amphiphilicity, softness, and degradability characteristics. This allows nanogels to encapsulate a wide variety of molecules, from inorganic molecules to biomacromolecules, while retaining their gel-like properties in circulation.[9] Nanogels made of amphiphilic-associating polymers incorporate the advantages of micelles (including an increase in solubility and half-life) but have higher stability than micelles.[42] Additional ways that nanogels achieve a longer half-life are by preventing the clearance of small molecules or by preventing quick degradation and metabolism of biomolecules.[9] Nanogels also effectively

improve the absorption of drugs with high molecular weights.[5] The combination of these properties makes nanogels ideal drug delivery systems for drugs with poor water solubility, low bioavailability, short circulation half-life, and severe adverse effects.[5]

One of the main benefits of nanogels is their ability to respond to environmental stimuli via the swelling and deswelling of the nanogel network.[43] Nanogels can be formulated to respond to several external signals, including acidity, temperature, hypoxia, reduction reaction within nanogels and surroundings, and enzyme-response stimuli. This stimulus sensitivity allows for site-specific and controlled release of loaded drugs and targeted delivery based on the properties of the targeted tissue.[42] The kinetics of drug release in nanogel systems depend greatly on environmental factors such as temperature, interactions between the loaded gel and the nanogel cross-linked network, and swelling or degradation of the nanogel network.[43] The linked matrices of nanogels enable them to retain their structure in circulation and promote increased drug release when exposed to a physiological stimulus.[5] Many nanogel systems are designed to have excellent pH sensitivity which is useful in targeting infected, inflamed, and malignant tissues that generally exhibit lower pH.[42] Other nanogels respond to redox balance in intracellular environments or expression levels of specific biomolecules as compared to normal physiological levels. Nanogel systems can also be designed to be multi-stimuli sensitive by responding to a combination of various extracellular signals to allow for a more site-specific response.[9]

These benefits of nanogels make it an ideal potential candidate for use in cancer therapy. The incorporation of nanogels into traditional chemotherapeutics limits common pitfalls patients experience by producing a more tumor-specific response based on the properties of cancer tissues along with controlled-release mechanisms. Nanogels also have a high potential for reversing drug resistance, which is a common occurrence in cancer monotherapies.[5]

Nanoparticles can be used for targeted drug delivery, but they require further optimization and research since each nanoparticle and drug combination must be evaluated for toxicity, longevity, efficacy, degradation, and scalability.[5]

Nanoparticles for Pancreatic Cancer Treatments

Various nanoparticle bound chemotherapy therapies have been approved for pancreatic cancer treatment. Examples include Abraxane® which was approved for clinical use as a first-line treatment in combination with the chemotherapeutic gemcitabine for metastatic pancreatic cancer in 2013 by the FDA.[44] Abraxane is made of bound paclitaxel (a chemotherapeutic) in nanoparticle-bound albumin (a protein produced by the liver).[45] Pancreatic cancer nanoparticle approved treatments expanded to Onivyde® when it was approved in 2015 by the FDA.[44] Onivyde® is used as a second-line treatment for metastatic pancreatic cancer in combination with 5-fluorouracil and leucovorin, and is made of a liposomal irinotecan.[44,45] Most recently, Pazenir® – another albumin/paclitaxel bound nanoparticle – was approved as a first-line treatment for metastatic pancreatic cancer in combination with gemcitabine by the EMA in 2019.[46] These approved examples of chemotherapy incorporated nanoparticles have paved the way for chemotherapy/nanoparticle based treatments for pancreatic cancer, demonstrating the efficacy of such treatments.

Unfortunately, the success of these treatments are limited. The ability to target pancreatic cancer sites is not improved with the use of nanoparticles, as these therapies still rely on the EPR effect to be deposited near a tumor. When looking at results of these therapies from clinical trials, Abraxane and gemcitabine combination therapy only increased overall survival to 8.5 months compared to 6.5 months of just gemcitabine treatment.[47] A recent clinical trial showed that the overall survival of Onivyde was 11.1 months.[48] While there is a slight improvement in the overall

survival of patients who have a nanoparticle chemotherapeutic treatment rather than a treatment with no drug carrier, there is still a lot of room for improvement as there is currently not treatment for pancreatic cancer that significantly reduces mortality.

NanoART631

While ART631 has been shown to be very effective and potent towards cancerous cells, it does have certain limitations such as short half life, low bioavailability, and cytotoxicity towards healthy cells. NanoART631 aims to improve upon these issues.

NanoART631 is a nanogel consisting of two cross-linked polymers, Dex-lactateHEMA macromer and Poly N-Isopropylacrylamide (PNIPAAM), that is copolymerized with ART631 as shown in Scheme 1. NanoART631 is a unique nanogel formulation that can change size based on temperature. ART631, a hydrophobic drug, is incorporated into the nanogel via UV emulsion in water. This allows for a very high loading capacity as compared to other methods of encapsulating hydrophobic drugs. Thus, NanoART631 can encapsulate artemisinin, sequester it, and then release it at or near cancerous tissue causing damaging effects to the tumor.

While this unique formulation has been studied in leukemia by Lowe Lab, little is known about the effects of NanoART631 on pancreatic cancer cells. Thus, this study aimed to evaluate the cell viability of PANC-1 cancer cells after exposure to NanoART631 in vitro and determine the physical size and makeup of NanoART631 to understand the viability of it as a pancreatic cancer treatment.

Chapter 3: Materials and Methods

Materials

NanoART631 nanoparticles containing 0, 2, 5, and 10 wt% ART631 were synthesized and received from Noha Ghonim in the Lowe Lab at the University of Maryland Baltimore School of Dentistry, Baltimore. Three mL semi-micro cuvettes were obtained from SARSTEDT AG & Co., Nümbrecht, Germany. The following materials were obtained from American Type Culture Collection (ATCC), Manassas, VA: Human pancreatic carcinoma cells (PANC-1), and Dulbecco's Modified Eagle's Medium (DMEM), MIA PaCa-2 cells. Human primary pancreatic epithelial cells (HPaMEC) were purchased from Cell Biologics along with the Complete Human Epithelial Cell Medium kit. The following materials were purchased from ThermoFisher Scientific, Nazareth, PA: fetal bovine serum (FBS), 25 cm^2 culture flasks with vented caps, 75 cm^2 culture flask with vented caps, GIBCO horse serum, phosphate buffered saline (PBS), trypsin-EDTA 0.25% with phenol red, Dimethyl Sulfoxide (DMSO), and penicillin‑streptomycin (pen-strep). 15 mL and 50 mL conical centrifuge tubes and 96-well microwell plates were obtained from Stellar Scientific, Baltimore, MD.
3-(4,5-Dimethylthiazol-2-yl)-2,5-Diphenyltetrazolium Bromide (MTT) powder was obtained from MilliporeSigma, Burlington, VT.

NanoART631 Characterization

Fourier-Transform Infrared Spectroscopy (FTIR)

NanoART631 containing 0 , 2, and 5 wt% ART631 as well as ART631 alone were also characterized by FTIR spectroscopy(Model:Thermo Electron Corporation Nicolet 6700) and

analyzed using OMNIC. A speck of each sample was placed on top of the diamond crystal and analyzed over a wavenumber range of 400-3600 cm^{-1}.

NanoART Particle Size and Zeta Potential in Water and Media

In preparation for Dynamic Light Scattering (DLS) 1 mg/mL samples of NanoART631 nanoparticles containing 0, 2, 5, and 10 wt% ART631 in powder form were prepared using sterile DI-water and complete cell media (PANC-1 and MIA PaCa-2) as the solute. 1 mL of the solution was added to a 3 mL semi-micro cuvette and placed into a Malvern Zetasizer Ultra. All samples were read three times at 37℃ and the water samples were additionally read three times at 25℃. Data was gathered via ZS Xplorer software and analyzed in Microsoft Excel.

Toxicity Studies

Cell Culture

PANC-1 were cultured in DMEM supplemented with 10% FBS and 1% pen-strep. The cells were grown in 25 cm^2 culture flasks with vented caps while incubated at 37°C with 5% CO2. Fresh cell culture media was replenished every 2 to 3 days, and cells were regularly monitored microscopically. Cells were passaged into a 75 cm^2 culture flask with vented caps when confluence reached 70 – 80% and further subcultured at a ratio of 1:2 once confluence was reached again.

MIA PaCa-2 cells were cultured in DMEM supplemented with 10% FBS, 2.5% horse serum, and 1% pen-strep. The cells were grown in 25 cm^2 culture flasks with vented caps while incubated at 37°C with 5% CO2 until confluent. Fresh cell culture media was replenished every 2 to 3 days, and cells were regularly monitored microscopically. Cells were passaged into a 75

cm^2 culture flask with vented caps when confluency reached 70 – 80% and further subcultured at a ratio of 1:2 once confluent was reached again.

HPaMEC cells were cultured in complete human epithelial cell medium which consisted of the basal medium supplemented with 5% FBS, 1% antibiotic-antimycotic solution, 0.1% hydrocortisone, and 0.1% epithelial growth factor. The cells were grown in 25 cm^2 culture flasks with vented caps coated in a 0.1% gelatin solution while incubated at 37°C with 5% CO2 until confluent. Fresh cell culture media was replenished every 2 to 3 days, and cells were regularly monitored microscopically. Cells were passaged into 75 cm^2 culture flasks with vented caps when confluency reached 70 – 80% and further subcultured at a ratio of 1:2 once confluent was reached again.

Cytotoxicity Study and IC_{50} *Determination*

The cytotoxic effect of NanoART631 on PANC-1 cells was determined using the MTT assay. The cells to be tested came from a T-75 cm^2 flask with confluent growth. 5 mL PBS was added to the flask, swished around gently, then aspirated. 2 mL trypsin-EDTA 0.25% with phenol red was added to the flask, and incubated for 2 minutes. Once out of the incubator, 4 mL cell culture media was added to the cells and pipetted up and down 6-8 times. Cells and media were then transferred to a 15 mL conical centrifuge tube from which 10 µL of cell/media solution was extracted for cell counting. The 15 mL conical tube was centrifuged at 130 RCF for 7 minutes. Once removed from the centrifuge, the supernatant was aspirated from the tube, leaving the cell pellet undisturbed. Then, 1 mL of cell culture media was added and pipetted up and down gently to break apart clumps in the pellet.

Using the 10 µL set aside earlier, the cells were counted to determine the total number of cells in the 15 mL conical tube. The volume V1 of media needed to bring the cell-media

concentration above 20 µL and to result in 20-50 µL volume V2 of cell solution in each well is determined. Volume (V1 - 1 mL of media previously added) is added to the 15 mL conical tube containing the cell-media solution.

Volume V2 of cells was plated into each well at 10,000 cells/well in 96-well microwell plates (Stellar Scientific, Baltimore) using a multichannel pipette. Additional media was added to each well to have a final volume of 100uL.100uL of media was added into the media-only control wells.

24 hours after the cells were seeded, three stock solutions of NanoART631 were prepared with nanogel concentrations of 50 mg/mL, 0.5 mg/mL, and 0.005 mg/mL. Using C1V1=C2V2, the volume of stock needed to create the desired nanogel concentrations was calculated. The calculated volume was removed from each well and replaced with the same volume of corresponding stock (Table 1). Four replicates of 10, 5, 1, 0.5, 0.05, 0.005, 0.001, 5e-4, and 5e-5 mg/mL were prepared. To react with the drug, cells were incubated at 37°C with 5% CO2 for 48 hours.

Table 1. Dilution Schema for all Nanogel concentrations and weight percentages.

Final Drug concentrations (mg/mL)	10	5	2	0.5	0.05	0.005	0.001	0.0005	0.00005
Amount of media removed from each well (uL)	20	5	2	1	10	1	0.2	10	1
Amount of stock solution added to each well (uL)	20uL of **50mg/ mL** stock solution	5uL of 50mg/ mL stock solution	2uL of 50mg/ mL stock solution	1uL of 50mg/ mL stock solution	10uLof **0.5mg/ mL** stock solution	1uLof 0.5mg/ mL stock solution	0.2uLof 0.5mg/ mL stock solution	10uL of **0.005 mg/mL** stock solution	1uL of 0.005 mg/mL stock solution

After 48 hours of incubation, 50 µL of MTT solution at a concentration of 5 mg/mL in PBS was added to each well and the cells were further incubated for three hours at 37°C in the

dark. 80% (or 120 µL)of the solution from each well was removed, leaving the formazan crystals formed undisturbed with approximately 30 µL media. 120 µL of DMSO was added to each well using a multichannel pipette and pipette up and down to dissolve the crystals. Absorbance is then measured at 570 nm in an absorbance reader.

The percentage of cell viability was calculated according to the following equation:

$$Cell\ viability\ (\%) = \frac{absorbance_{treated\ cells} - absorbance_{media}}{absorbance_{untreated\ cells} - absorbance_{media}} \times 100$$

The IC_{50} value was calculated as the concentration of the 0 wt%, 2 wt%, 5 wt%, and 10 wt% NanoART631 needed to reduce the cell viability of treated cells to 50% compared with control.

Statistical Analysis

The nanoparticle characterization data was analyzed using the Student's t-test which was used as the condition to indicate a statistically significant difference. Data points were compared whenever one parameter was changed. The parameters being manipulated were the wt% ART631 content, temperature, and suspension of the particles in water or cell media. A significant difference was defined as a p value less than 0.05.

The cytotoxicity results are graphed as the mean with error bars set as ± one standard deviation of quadruplicate cultures. Outliers were removed; they were identified as further from the median than ± three median absolute deviations (MAD).[49] To calculate the IC_{50}s, the log(inhibitor) vs. response - Variable slope (four parameters) model was used on GraphPad Prism (v10.2.2). The model was fit to the entire data set plus the negative control, which was set to a low concentration of 10^{-6} mg/mL in the fitting software, because $\log_{10}0$ is undefined.

Chapter 4: Results

NanoART631 Characterization

FTIR and dynamic light scattering (DLS) were used to characterize the chemical structure and physical property including hydrodynamic diameter and polydisperse index (PDI) of NanoART631s containing ART631 at 0, 2, and 5 wt%.

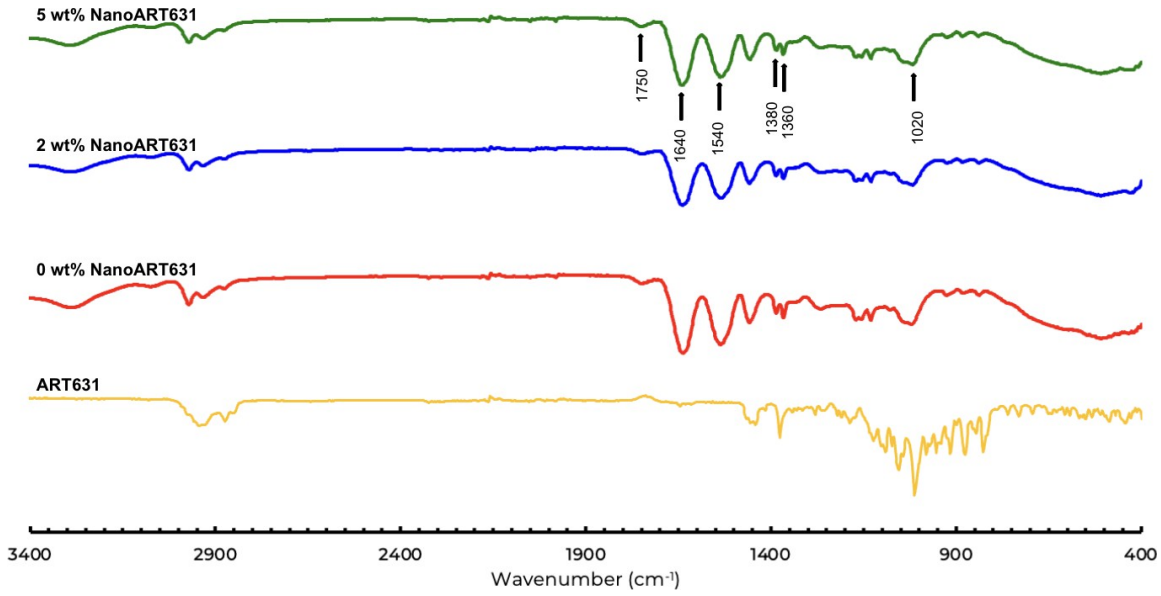

Figure 1. FTIR Spectra of ART631 and NanoART631s containing ART631 0, 2, and 5 wt%.

Figure 2 showed the FTIR spectra of the ART631, the nanogels alone and NanoART631s containing 2 and 5 wt% ART631. Both the spectra of NanoART631s displayed the characteristic bands of Dex-lactateHEMA at 1750 (C=O stretching from the lactateHEMA group) and 1010 cm^{-1} (C-OH stretching from the dextran group). Additionally, Amide I and II bands appeared at 1640 and 1540 cm^{-1}, respectively, and symmetric C-H bending from the $–CH(CH_3)_2$ group of PNIPAAM appeared at 1380 and 1360 cm^{-1}. These values were confirmed by literature sources.[43] Furthermore, the peak intensity at 1010 cm^{-1} normalized by that at 1640 cm^{-1} increased with increasing the weight percent of ART631 in NanoART631s from 0 to 5 wt% (Table 2). These

FTIR results suggested that ART631 was successfully incorporated into the nanogels.

Table 2. Ratios of the FTIR peak intensities of NanoART631s at wavenumbers 1020 and 1640 cm^{-1}.

	Ratio of FTIR Peak Intensity Increase
0 wt% NanoART631	0.63
2 wt% NanoART631	0.65
5 wt% NanoART631	0.69

DLS measurements then provided insight into the size of our synthesized nanogel drug molecules and their dispersity in particle size (Tables 3-4). To determine dispersity within our particle size, we also used the DLS to determine the polydispersity index of NanoART631 amongst its formulations (Tables 3-4). Furthermore, to evaluate the stability of the nanogel dispersion, the zeta potential was measured for a NanoART631 suspension in both water and cell media.

Table 3. Hydrodynamic diameters, PDIs, and Zeta Potentials of NanoART631s dispersed in water at 25 and 37℃. Three replicates were performed and data are represented as mean ± standard deviation.

	Diameter (nm) at 25℃	PDI at RT	Zeta Potential (mV) at RT	Diameter (nm) at 37℃	PDI at 37 ℃	Zeta Potential (mV) at 37 ℃
0 wt% NanoART631	134.4 ± 22.7	0.64 ± 0.06	-9.42 ± 0.64	171.3 ± 10.0	0.08 ± 0.02	-12.19 ± 0.35
2 wt% NanoART631	211.9 ± 4.2	0.12 ± 0.01	-12.19 ± 1.64	143.0 ± 5.5	0.06 ± 0.00	-15.95 ± 0.81
5 wt% NanoART631	259.6 ± 0.9	0.10 ± 0.02	-9.91 ± 7.48	189.7 ± 30.3	0.08 ± 0.02	-16.91 ± 0.40
10 wt% NanoART631	307.0 ± 4.0	0.07 ± 0.00	-7.00 ± 8.12	227.2 ± 15.0	0.23 ± 0.02	-11.07 ± 0.11

Table 4. Hydrodynamic diameters, PDIs, and Zeta Potentials of NanoART631s dispersed in MIA PaCa-2 and PANC-1 culture media at 37℃. Three replicates were performed and data are represented as mean ± standard deviation.

	MIA PaCa-2 Media			PANC-1 Media		
	Diameter (nm) at 37	PDI at 37℃	Zeta Potential	Diameter (nm) at 37	PDI at 37℃	Zeta Potential
0 wt% NanoART631	133.5 ± 2.2	0.04 ± 0.03	-1.13 ± 0.90	126.6 ± 3.0	0.03 ± 0.01	-0.85 ± 0.91
2 wt% NanoART631	112.4 ± 2.8	0.06 ± 0.04	-1.66 ± 0.63	113.5 ±1.7	0.04 ± 0.01	-4.19 ± 0.37
5 wt% NanoART631	118.9 ± 2.2	0.11± 0.02	-0.11 ± 1.65	119.5 ± 2.6	0.11 ± 0.02	-0.52 ± 1.07
10 wt% NanoART631	135.6 ± 4.0	0.23 ± 0.01	2.35 ± 2.66	147.1 ± 10.9	0.24 ± 0.01	1.81 ± 2.19

Table 5. Statistical analysis of hydrodynamic diameters of NanoART631s dispersed in water at 25 ℃ and 37 ℃ and in MIA PaCa-2 and PANC-1 culture media at 37 ℃. P-values calculated using Student's T-Test and N=3 for all comparisons.

	0 wt% vs. 2 wt%	0 wt% vs. 5 wt%	0 wt% vs. 10 wt%	2 wt% vs. 5 wt%	2 wt% vs. 10 wt%	5 wt% vs. 10 wt%
25℃ water	0.02	0.01	0.005	0.004	0.0003	0.004
37℃ water	0.051	0.51	0.06	0.13	0.01	0.07
37℃ PANC-1 media	0.003	0.005	0.07	0.009	0.03	0.04
37℃ MIA PaCa-2 media	0.003	0.03	0.48	0.12	0.02	0.03

	0 wt%	2 wt%	5 wt%	10 wt%
25℃ water vs. 37℃ water	0.19	0.006	0.06	0.01
37℃ water vs. 37℃ PANC-1 media	0.03	0.009	0.05	0.005
37℃ water vs. 37℃ MIA PaCa-2 media	0.03	0.02	0.06	0.007
37℃ PANC-1 media vs. 37℃ MIA PaCa-2 media	0.03	0.60	0.84	0.25

Table 6. Statistical analysis of polydispersity of NanoART631s dispersed in MIA PaCa-2 and PANC-1 culture media at 37 ℃ and water at 25 ℃ and 37 ℃. P-values calculated using Student's T-Test and N=3 for all comparisons.

	0 wt% vs. 2 wt%	0 wt% vs. 5 wt%	0 wt% vs. 10 wt%	2 wt% vs. 5 wt%	2 wt% vs. 10 wt%	5 wt% vs. 10 wt%
25℃ water	0.004	0.004	0.003	0.24	0.0004	0.10
37℃ water	0.31	0.92	0.0001	0.34	0.005	0.03
37℃ PANC-1 media	0.89	0.002	0.005	0.05	0.0004	0.02
37℃ MIA PaCa-2 media	0.57	0.059	0.01	0.32	0.01	0.02

	0 wt%	2 wt%	5 wt%	10 wt%
25℃ water vs. 37℃ water	0.004	0.00006	0.002	0.007
37℃ water vs. 37℃ PANC-1 media	0.11	0.09	0.21	0.31
37℃ water vs. 37℃ MIA PaCa-2 media	0.28	0.96	0.25	0.97
37℃ PANC-1 media vs. 37℃ MIA PaCa-2 media	0.80	0.34	0.14	0.053

Table 7. Statistical analysis of zeta potential of NanoART631s dispersed in MIA PaCa-2 and PANC-1 culture media at 37 ℃ and water at 25 ℃ and 37 ℃. P-values calculated using Student's T-Test and N=3 for all comparisons.

	0 wt% vs. 2 wt%	0 wt% vs. 5 wt%	0 wt% vs. 10 wt%	2 wt% vs. 5 wt%	2 wt% vs. 10 wt%	5 wt% vs. 10 wt%
25℃ water	0.13	0.92	0.64	0.71	0.45	0.02
37℃ water	0.04	0.005	0.007	0.11	0.01	0.001
37℃ PANC-1 media	0.02	0.76	0.10	0.046	0.03	0.33
37℃ MIA PaCa-2 media	0.55	0.56	0.23	0.22	0.12	0.06

	0 wt%	2 wt%	5 wt%	10 wt%
25℃ water vs. 37℃ water	0.01192045	0.032446	0.24963	0.472759
37℃ water vs. 37℃ PANC-1 media	0.0008	0.003	0.0006	0.009
37℃ water vs. 37℃ MIA PaCa-2 media	0.004	0.001	0.003	0.01
37℃ PANC-1 media vs. 37℃ MIA PaCa-2 media	0.81	0.046	0.77	0.60

The diameters of NanoART631s ranged from 134 to 307 nm at 25 ℃, with the smaller size being the 0 wt% and the larger being the 10 wt%. At 37 ℃, the sizes range from 171.3 nm to 227.2 with the same pattern. When looking at the diameter of NanoART631 dissolved in water (Table 3), we notice that at 25 ℃, the diameter increases as the ART631 amount increases. However, that is not the trend that we see at 37 ℃. Instead, we see that the NanoART631 0 wt% formulation has a larger diameter than the NanoART631 2 wt% formulation at 37℃, and then size again increases by ART631 amount. In water, our NanoART631 formulations shrink at higher temperatures than at lower temperatures, with the only exception being the 0 wt%, where the particle size increases with increasing temperature. According to Table 4, our NanoART631 formulations are smaller in size when they are in cell medium at 37 degrees Celsius. Not much difference in size is noticed between our formulations in MIA PaCa-2 cell culture media versus in PANC-1 cell culture media.

Overall, the PDIs of the NanoART631s in both water and cell media at body temperature were below 0.25, indicating the NanoART631s were monodisperse. At room temperature, the PDIs were also low except for at 0 wt%, where the population is relatively polydisperse at 0.64.

In both cell media, the PDI is also consistently below 0.25 at body temperature for all weight percentages.

In water, the zeta potential of all the NanoART631s containing ART631 at 0, 2, 5 and 10 wt% were all negative with values below 20 mV at both 25 and 37 °C. At 37 °C in water, the zeta potential value increased with increasing the amounts of ART631 from 0 to 2 to 5 wt%, but started to decrease when the ART631 reached 10 wt%. However, in water at 25 °C and in the cell media at 37 °C, the zeta potential increased with 0 wt% to 2 wt% ART631 and then decreased at 5 wt% and even less negative at 10 wt%. The cell culture media decreased the zeta potential value due to the presence of salts in the cell culture media. Similarly, in both types of cell media, the magnitude of zeta potential was less than 5 mV for all the NanoART631s.

Cytotoxicity Study and IC_{50} Determination

Next, in efforts to analyze the effects of our nanogel with and without drug, MTT trials were performed with 0 wt%, 2 wt%, 5 wt%, and 10 wt% NanoART631 on a 48-hour timescale (Figures 2-3).

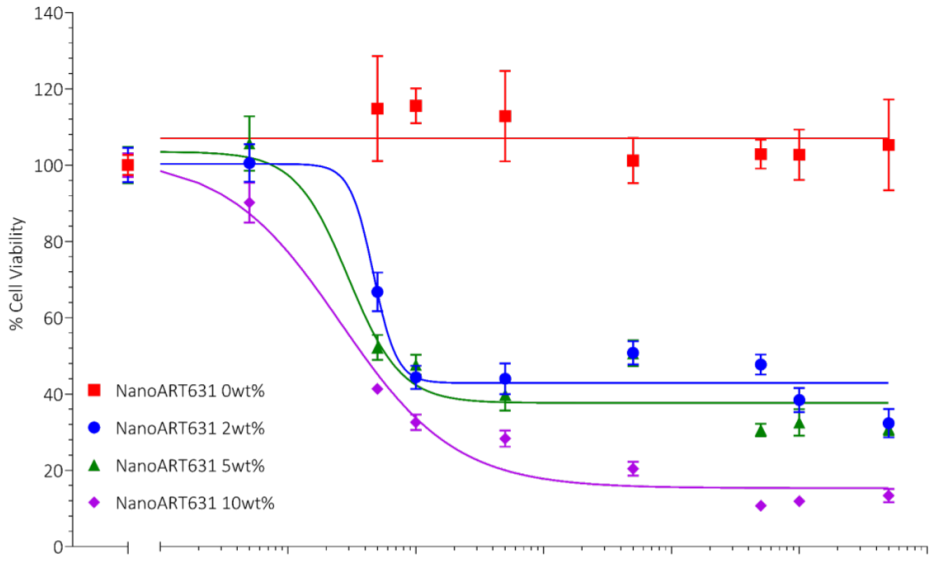

Nanogel Concentrations (mg·mL^{-1})	0	0.0001	0.001	0.01	0.1	1	10
2wt% ART631 (nM)	0	3.169	31.69	316.96	3169.57	31695.7	316957
5wt% ART631 (nM)	0	7.924	79.24	792.39	7923.93	79239.3	792393
10wt% ART631 (nM)	0	15.848	158.48	1584.79	15847.86	158478.6	1584786

Figure 2. MTT assay of 0 wt%, 2 wt%, 5 wt%, and 10 wt% NanoART631 on MIA PaCa-2 cells. All trials were performed on a 48-hour timescale.

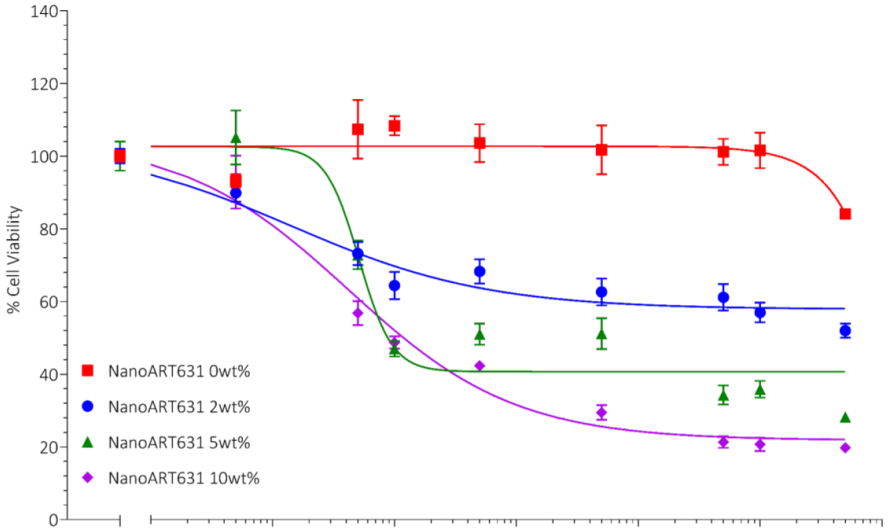

Nanogel Concentrations (mg·mL^{-1})	0	0.0001	0.001	0.01	0.1	1	10
2wt% ART631 (nM)	0	3.169	31.69	316.96	3169.57	31695.7	316957
5wt% ART631 (nM)	0	7.924	79.24	792.39	7923.93	79239.3	792393
10wt% ART631 (nM)	0	15.848	158.48	1584.79	15847.86	158478.6	1584786

Figure 3. MTT assay of 0 wt%, 2 wt%, 5 wt%, and 10 wt% NanoART631 on PANC-1 cells. All trials were performed on a 48-hour timescale

An IC_{50} for both cell lines was determined for each wt% tested (Table 8).

Table 8: IC_{50}s from cytotoxicity study of NanoART631 at various drug percentages on PANC-1 and MIA PaCa-2 (with r^2 values to describe goodness of fit to 4-parameter logistic model)

Cell Line	Sample	IC50 (μg/mL)	IC50 (nM) Theoretical	Yield (%)	IC50 (nM) Actual
PANC-1	NanoART631 2wt%	N/A	N/A	86.59	N/A
	NanoART631 5wt%	0.8820	69.89	92.69	64.78
	NanoART631 10wt%	1.1883	188.32	86.00	161.96
MIA PaCa-2	NanoART631 2wt%	0.7027	22.27	86.59	19.29
	NanoART631 5wt%	0.5946	47.12	92.69	43.67
	NanoART631 10wt%	0.3919	62.11	86.00	53.41

Chapter 5: Discussion

NanoART631 characterization was performed to understand and analyze NanoART631's efficacy in the human body as a drug carrier. The chemical structure was determined through FTIR analysis and provided confirmation of synthesized gels. All structural components determined through FTIR corroborated the current literature.[43]

As seen in Table 3, 25 °C diameters of the 2, 5, and 10 wt% NanoART631 were larger than their corresponding diameters at 37 ℃, while the 25 ℃ diameter of the 0 wt% was significantly smaller than that at 37 ℃ ($p < 0.5$). Previous literature published by the Lowe Lab corroborates that the lower critical solution temperature (LCST) of this nanogel is at 32 ℃. Therefore, the trend we see happening here is consistent. A current hypothesis to explain the increase in size of 0 wt% NanoART631 is that higher temperatures cause more aggregation of the nanogel resulting in larger hydrophobic segments of the nanoparticle and therefore an increase in diameter. A potential explanation for the smaller diameters at higher temperatures is that the NIPAAM polymers tend to shrink at higher temperatures. It is possible that both scenarios are occurring at once, and there is a tradeoff in the outcome depending on the percent weight of the NanoART631. The particle sizes decreased with increasing ART631 amount from 0 to 2 wt% and then increased with increasing ART631 amount from 2 to 10 wt% due to the hydrophobicity of ART631, but there is no statistical significance from this trend. Therefore, further trials are in order to determine how temperature affects NanoART631 at varying ART631 percent loading weights.

The hydrodynamic size of our nanogel formulations in MIA PaCa-2 media and PANC-1 media at 37 ℃ (seen in Table 4) shows a similar trend as the particle size in water at 37 ℃. In PANC-1 media, The particle sizes decreased with increasing ART631 amount from 0 to 2 wt%

($p = 0.003$) due to the hydrophobicity of ART631 and then increased with increasing ART631 amount from 2 to 10 wt% ($p < 0.3$). In MIA PaCa-2 media, the particle size significantly decreased from 0 to 2 wt% and increased from 5 to 10 wt% like in PANC-1 media, but there was no significant change in particle size from 2 to 5 wt%. However, the overall sizes of the nanoparticles were significantly smaller in cell media than in water at 37 ℃ ($p < 0.5$). This is due to the higher concentration of salts in the cell media interacting with the hydrophobicity of the nanogels and causing them to shrink. No statistical difference was seen between particle sizes in MIA PaCa-2 media and PANC-1 media except for the 0 wt% formulation, where 0 wt% NanoART631 was smaller in PANC-1 media than in MIA PaCa-2 media ($p=0.026$).

The PDI values calculated show that at body temperature, NanoART631 is monodisperse, indicating good quality of the formulation. Monodispersity is beneficial for accurately testing the stability and the quality of the nanogel, as low distribution describes a more uniform sample with respect to particle size.[50] The PDI of NanoART631 at body temperature (37℃) was below 0.23 for all formulations. This indicates that at biological temperatures, NanoART631 is primarily monodisperse. NanoART631 shows promise to be effective in practice based on its size and monodispersity at the body's temperature.[50]

The zeta potential data in Table 3 shows that the addition of 2 wt% ART631 into the nanogels suspended in water at 37 °C resulted in the zeta potential becoming more negative ($p = 0.04$), with no significant change at 25 °C. When the ART631 content increased to 5 wt%, the zeta potential decreased (but not significantly) at both temperatures. With the further increase of ART631 loading from 5 to 10 wt%, the zeta potential value decreased at both temperatures($p < 0.02$). The zeta potential became more negative when temperature was increased from 25 to 37 °C but there is not a significant change in the 5 and 10 wt% formulations. The possible

explanations for the zeta potential changes based on ART631 loading amount is thatART631 is slightly negative and hydrophobic. More negative charges decreases the zeta potential, and the hydrophobicity increases the particle size and thus decreases the zeta potential value. The increase of the zeta potential values due to temperature was probably because the particle size decreased with increasing the temperature except for the nanogels alone without ART631. The zeta potential of the nanogels alone became more negative even though the particle size increased when temperature was increased from 25 to 37 °C probably because higher temperature broke the ester bond of nanogels faster causing more carbolic acid present on the nanogels and thus making the nanogels being more negative.

When the NanoART631s were dispersed in the culture media for the two PANC-1 and MIA PaCa-2 cell lines instead of DI water, the zeta potential values (Table 4) significantly decreased closer to 0 mV compared to NanoART631 in water probably due to the salting out effect of the salts and proteins in the culture media ($p < 0.01$). Statistically, there is no obvious comparison between the change in zeta potential of NanoART631 with increasing ART631 content in water and media. However, they do follow the same general trend of the zeta potential being more negative as lower amounts of ART631 content are added and then decreasing at 10 wt%. There is no statistical significance in the zeta potential of NanoART631 in MIA PaCa-2 and PANC-1 media suggesting that the differences in composition of the two cell culture media did not have much effect on the zeta potential.

Before testing the efficacy of NanoART631, it was important to categorize the effect of the nanogel alone on the cancer cell lines to see if the nanogel itself is toxic to cells. To do so, MTT assays were performed on the PANC-1 and MIA PaCa-2 cell lines with 0 wt% of NanoART631, the nanogel with no drug loaded. With PANC-1 cells, there is above 100%

viability up to 0.5 mg/mL of 0 wt% NanoART631 (Figure 3). MIA PaCa-2 follows a similar trend with above 100% viability between 0.001 and 1 mg/mL concentrations (Figure 2). It is not entirely clear why there is above 100% viability, but this finding does corroborate previous findings from Noha Gohmin at Lowe Lab with other cancer cell types where they also saw the nanogel alone increase cell viability above 100% for a certain range of concentrations.

The 0 wt% nanogel formulation did not have any IC_{50} values, meaning that it was not able to kill 50% of our cancer cells, even at high concentrations. Furthermore, for both MIA PaCa-2 and PANC-1 cell lines, cell viability remained over 80% (and mostly 100%) when NanoART631 0 wt% was added to the cells. This further indicates that the nanogel alone does not contribute to the toxicity of the formulation and that ART631 is the sole cytotoxic component that kills the cancer cells, especially at lower concentrations. We determined that the nanogel is a safe carrier at the concentrations where this drug would be administered, isolating the cause of any potential cell death at low concentrations to be the ART631, rather than the nanogel.

The IC_{50}s determined in our results are very promising. NanoART631 2, 5 and 10 wt% have nanoMolar concentration values for MIA PaCa-2 cells (Table 8). No IC_{50} value was determined from NanoART631 2 wt% on PANC-1 cells, but the 5 and 10 wt% formulations did result in IC_{50} values in the nanoMolar concentration. Figure 2 and 3 show that percent cell viability decreased with increasing wt% of ART631 encapsulated in NanoART631. With increasing nanogel concentration, NanoART631 10 wt% was able to kill more than 80% of both MIA PaCa-2 and PANC-1 cells, while 5 wt% was able to kill more than 60% and 2 wt% was able to kill around 50%. This demonstrates that increasing the wt% of ART631 in NanoART631 is more successful at inhibiting cell growth across the two pancreatic cancer cell lines tested, and therefore less drug is needed to achieve the same loss in cancerous cell viability.

At the same time, we see that the actual IC_{50} values increase as ART631 wt% increases. For example, when treating MIAPaCa-2 cells with NanoART631 2 wt%, only 19.29 nM of ART631 was sufficient at killing 50% of MIA PaCa-2 cells. However, the NanoART631 5 and 10 wt% formulations resulted in IC_{50} values of 43.67 and 53.41 nM respectively. We see a similar trend for PANC-1 cells, where the IC_{50} increases with increasing wt% (64.78 nM for 5 wt% and 161.96 nM for 10 wt%). It is believed that this trend is due to cell uptake. We hypothesize that the cells are only able to intake a certain amount of nanogel rather than the entire administered dose. The NanoART631 formulations with higher wt% of ART631 will deposit more ART631 inside the cells than lower wt % which results in a higher IC_{50} value.

When comparing the cytotoxic effect of NanoART631between cell lines, PANC-1 cell line is more resistant to treatment than MIA Paca-2. NanoART631 2 wt% was not able to kill 50% of PANC-1 cells but was able to for MIA PaCa-2 cells, and the IC_{50} of 5 and 10 wt% are higher for PANC1 cells than MIA PaCa-2 cells. Each cell line is representative of a form of pancreatic cancer from one individual, so anyone can have different sensitivities to treatment. Importantly, although PANC-1 was more resistant to treatment than MIA PaCa-2, both cell lines had significantly inhibited cell viability as a result of increasing weight percentages of NanoART631, demonstrating that the treatment is effective against all pancreatic cancer cell lines tested.

Future Directions

There are many directions for this research to be expanded on in the future. This study focused on using MTT to measure cytotoxicity and determine an IC_{50} for two cell lines. Other cell assays and cellular uptake studies could be used to expand on the findings in this paper.

Future directions of this study should also focus on testing other cell lines that vary in location within the pancreas, stage of cancer, and demographics of the individual who donated the cells. Importantly, NanoART631 also should be tested on healthy pancreatic cells to determine whether this drug is safe to use in humans and to confirm that it in fact targets cancer cells over healthy cells. Promising results would demonstrate high inhibition of cell viability of cancerous cell lines with little to no loss in cell viability in the healthy cells. From there, apoptosis studies should be conducted in order to measure the actual self regulated cell death instead of metabolic activities. Uptake studies would demonstrate how much of the active component (ART631) gets taken up by the cells. With the groundwork laid with these studies, organoid studies could be a next step in order to depict a more accurate representation of what this treatment process would look like inside a pancreas, while still conducting *in vitro* studies. Finally, *in vivo* pharmacokinetics and therapeutic effects studies could be conducted to understand how NanoART631 would move throughout the body and what unknown side effects may accompany this treatment.

Chapter 6: Equity Impact

Cancer is among one of the deadliest diseases and treatment is burdensome for patients. One of the factors that contributes to the difficulty of treatment of cancers is pain management. Kemp and Kwon found that 55% of those doing treatment and 66% of patients with advanced cancer express that they experience high pain levels.[51] The high toxicity of common chemotherapeutic agents results in harmful impacts on the body since chemotherapeutic drugs damage both healthy and cancerous cells. However, early detection of cancer can allow for a higher five-year survival rate and lower cost of treatment for the patient.[51] Due to the higher usage of drugs in general, the novelty of treatment has decreased for patients and many develop

drug resistance to chemotherapeutic drugs.[51] Nanotechnology can alleviate the acquired resistance that humans have gained throughout their lifetime. On a larger scale, nanotechnology is addressing these issues by increasing early detection, targeted treatment, and management of pain.

The current treatment for pancreatic cancer can be taxing in itself and may have severe side effects that can include hair loss, nausea, vomiting, changes in appetite, and fatigue. These side effects are not only taxing for the patient themselves, but also to the family and friends of this patient who watch their loved one suffer. Pancreatic cancer treatment places a higher emphasis on chemotherapeutic treatments due to a typically late-stage diagnosis, thus making surgery less viable. Creating a more effective and efficient treatment is the most straightforward way to improve prognosis. NanoART631 is a promising therapeutic with a significant impact on cancerous cells and a limited effect on healthy pancreatic cells. The low toxicity of artemisinin could help remove the painful and tiring side effects of current treatments, thus improving the quality of life of patients.[7] This novel treatment is a promising way to consume and use the drug responsibly. As using a nanogel improves the delivery of the drug to the cancer site, less drug is lost en route to the pancreas, resulting in less drug waste in the system. The targeted drug delivery of the NanoART631 allows a significantly lower amount of drug to be used when combined with a nanogel which can decrease waste and decrease the harm to healthy cells of humans.

The burden of cancer is more than just the disease itself. In addition to the financial strain this illness brings upon many families, there is also a burden that arises from the extensive amount of time required for treatment. With NanoART631's shortened half-life, the drug stays in the body longer, requiring fewer doses. Thus, patients would require less frequent visits to

receive treatment. Not only would a more effective treatment increase the lifespans and quality of life for the patients, but it would also result in fewer visits that take away from time in the workplace and home.

Bibliography

1. Lei F, Xi X, Batra SK, Bronich TK. Combination Therapies and Drug Delivery Platforms in Combating Pancreatic Cancer. *J Pharmacol Exp Ther*. 2019;370(3):682-694. doi:10.1124/jpet.118.255786
2. Cancer.Net Editorial Board. Pancreatic Cancer: Statistics. https://www.cancer.net/cancer-types/pancreatic-cancer/statistics#:~:text=The%20disease%20accounts%20for%20approximately,year%20since%20the%20late%201990s
3. American Cancer Society. Pancreatic Cancer Facts. Published online 2023. https://pancreatic.org/pancreatic-cancer/pancreatic-cancer-facts/
4. Post E. Five-Year Pancreatic Cancer Survival Rate Increases to 12%. Pancreatic Cancer Action Network. Published January 12, 2023. https://pancan.org/news/five-year-pancreatic-cancer-survival-rate-increases-to-12/#:~:text=American%20Cancer%20Society%27s%20Cancer%20Facts,percentage%20point%20from%20last%20year
5. Attama AA, Nnamani PO, Onokala OB, Ugwu AA, Onugwu AL. Nanogels as target drug delivery systems in cancer therapy: A review of the last decade. *Front Pharmacol*. 2022;13:874510. doi:10.3389/fphar.2022.874510
6. Cheng Z, Li M, Dey R, Chen Y. Nanomaterials for cancer therapy: current progress and perspectives. *J Hematol OncolJ Hematol Oncol*. 2021;14(1):85. doi:10.1186/s13045-021-01096-0
7. Ghonim NA, Tabassum S, Mott BT, et al. Biodegradable Nanogels for Controlled Release of Artemisinin-derived Drug to Treat Leukemia. Published online 2022.
8. Wang J, Xu C, Wong YK, et al. Artemisinin, the Magic Drug Discovered from Traditional Chinese Medicine. *Engineering*. 2019;5(1):32-39. doi:10.1016/j.eng.2018.11.011
9. Soni KS, Desale SS, Bronich TK. Nanogels: An overview of properties, biomedical applications and obstacles to clinical translation. *J Controlled Release*. 2016;240:109-126. doi:10.1016/j.jconrel.2015.11.009
10. Ma Z, Woon CYN, Liu CG, et al. Repurposing Artemisinin and its Derivatives as Anticancer Drugs: A Chance or Challenge? *Front Pharmacol*. 2021;12. doi:10.3389/fphar.2021.828856
11. Lowe TL, Kim YS, Huang X. Multi-functional polymeric materials and their uses. *US20050169882A1*. https://patents.google.com/patent/US20050169882A1/en?oq=8545830. Published August 4, 2005.
12. Lowe TL, Civin CI. Platform nanoparticle technology for sustained delivery of hydrophobic drugs.
13. Meshnick SR. Artemisinin antimalarials: mechanisms of action and resistance. *Med Trop Rev Corps Sante Colon*. 1998;58(3 Suppl):13-17.
14. Guo Q, Li L, Hou S, et al. The Role of Iron in Cancer Progression. *Front Oncol*. 2021;11. Accessed February 20, 2023. https://www.frontiersin.org/articles/10.3389/fonc.2021.778492
15. Vareedayah AA, Alkaade S, Taylor JR. Pancreatic Adenocarcinoma. *Mo Med*. 2018;115(3):230-235.
16. Pancreatic Cancer Types. Johns Hopkins Medicine. https://www.hopkinsmedicine.org/health/conditions-and-diseases/pancreatic-cancer/pancreatic-cancer-types
17. Torti SV, Manz DH, Paul BT, Blanchette-Farra N, Torti FM. Iron and Cancer. *Annu Rev Nutr*. 2018;38(1):97-125. doi:10.1146/annurev-nutr-082117-051732
18. Crespo-Ortiz MP, Wei MQ. Antitumor Activity of Artemisinin and Its Derivatives: From a Well-Known Antimalarial Agent to a Potential Anticancer Drug. *J Biomed Biotechnol*. 2012;2012:1-18. doi:10.1155/2012/247597

19. Pancreatic Cancer Prognosis. Johns Hopkins Medicine. https://www.hopkinsmedicine.org/health/conditions-and-diseases/pancreatic-cancer/pancreatic-cancer-prognosis
20. Whipple Procedure. Johns Hopkins Medicine. https://www.hopkinsmedicine.org/health/conditions-and-diseases/pancreatic-cancer/whipple-procedure
21. Pancreatic Cancer Surgery. Johns Hopkins Medicine. https://www.hopkinsmedicine.org/health/conditions-and-diseases/pancreatic-cancer/pancreatic-cancer-surgery
22. Lopez M, Parreco J, Buicko J, Rishi R, Billingsley K, Castillo A. The true cost of high volume whipple procedures. *HPB*. 2018;20:S45-S46. doi:10.1016/j.hpb.2018.02.248
23. Radiation Therapy for Pancreatic Cancer. American Cancer Society. Published February 11, 2019. https://www.cancer.org/cancer/types/pancreatic-cancer/treating/radiation-therapy.html
24. Ellison L. Pancreatic Cancer Treatment Costs. American Life Fund. Published September 12, 2022. https://www.americanlifefund.com/cancer/treatment/costs/pancreatic/#:~:text=Radiation%20therapy%20averages%20about%20%249%2C000,when%20deciding%20on%20their%20healthcare
25. Yousaf MN, Ehsan H, Muneeb A, et al. Role of Radiofrequency Ablation in the Management of Unresectable Pancreatic Cancer. *Front Med*. 2021;7:624997. doi:10.3389/fmed.2020.624997
26. American Cancer Society Editorial Team. Chemotherapy for Pancreatic Cancer. American Cancer Society.
27. Hirsch J, Dieguez G, Cockrum P. Comparing total cost of care for Medicare FFS patients with pancreatic cancer by chemotherapy regimen. *J Clin Oncol*. 2020;38(15_suppl):e19394-e19394. doi:10.1200/JCO.2020.38.15_suppl.e19394
28. Mott BT, He R, Chen X, et al. Artemisinin-derived dimer phosphate esters as potent anti-cytomegalovirus (anti-CMV) and anti-cancer agents: A structure–activity study. *Bioorg Med Chem*. 2013;21(13):3702-3707. doi:10.1016/j.bmc.2013.04.027
29. Kagan AB, Moses BS, Mott BT, et al. A Novel 2-Carbon-Linked Dimeric Artemisinin With Potent Antileukemic Activity and Favorable Pharmacology. *Front Oncol*. 2022;11:790037. doi:10.3389/fonc.2021.790037
30. Mg K, V K, F H. History and Possible Uses of Nanomedicine Based on Nanoparticles and Nanotechnological Progress. *J Nanomedicine Nanotechnol*. 2015;06(06). doi:10.4172/2157-7439.1000336
31. Murthy SK. Nanoparticles in modern medicine: state of the art and future challenges. *Int J Nanomedicine*. 2007;2(2):129-141.
32. Khan I, Saeed K, Khan I. Nanoparticles: Properties, applications and toxicities. *Arab J Chem*. 2019;12(7):908-931. doi:10.1016/j.arabjc.2017.05.011
33. Bazak R, Houri M, El Achy S, Kamel S, Refaat T. Cancer active targeting by nanoparticles: a comprehensive review of literature. *J Cancer Res Clin Oncol*. 2015;141(5):769-784. doi:10.1007/s00432-014-1767-3
34. Mosquera J, García I, Liz-Marzán LM. Cellular Uptake of Nanoparticles versus Small Molecules: A Matter of Size. *Acc Chem Res*. 2018;51(9):2305-2313. doi:10.1021/acs.accounts.8b00292
35. Bélteky P, Rónavári A, Zakupszky D, et al. Are Smaller Nanoparticles Always Better? Understanding the Biological Effect of Size-Dependent Silver Nanoparticle Aggregation Under Biorelevant Conditions. *Int J Nanomedicine*. 2021;Volume 16:3021-3040. doi:10.2147/IJN.S304138
36. Huo S, Jin S, Ma X, et al. Ultrasmall Gold Nanoparticles as Carriers for Nucleus-Based Gene Therapy Due to Size-Dependent Nuclear Entry. *ACS Nano*. 2014;8(6):5852-5862.

doi:10.1021/nn5008572
37. Sukhanova A, Bozrova S, Sokolov P, Berestovoy M, Karaulov A, Nabiev I. Dependence of Nanoparticle Toxicity on Their Physical and Chemical Properties. *Nanoscale Res Lett*. 2018;13(1):44. doi:10.1186/s11671-018-2457-x
38. Kalyane D, Raval N, Maheshwari R, Tambe V, Kalia K, Tekade RK. Employment of enhanced permeability and retention effect (EPR): Nanoparticle-based precision tools for targeting of therapeutic and diagnostic agent in cancer. *Mater Sci Eng C*. 2019;98:1252-1276. doi:10.1016/j.msec.2019.01.066
39. Gratton SEA, Ropp PA, Pohlhaus PD, et al. The effect of particle design on cellular internalization pathways. *Proc Natl Acad Sci*. 2008;105(33):11613-11618. doi:10.1073/pnas.0801763105
40. Bullis K. Shape Matters for Nanoparticles. Technology Review. Published August 7, 2008. https://www.technologyreview.com/2008/08/07/33862/shape-matters-for-nanoparticles/
41. Fröhlich E. The role of surface charge in cellular uptake and cytotoxicity of medical nanoparticles. *Int J Nanomedicine*. Published online November 2012:5577. doi:10.2147/IJN.S36111
42. Zhang H, Zhai Y, Wang J, Zhai G. New progress and prospects: The application of nanogel in drug delivery. *Mater Sci Eng C*. 2016;60:560-568. doi:10.1016/j.msec.2015.11.041
43. Huang X, Lowe TL. Biodegradable Thermoresponsive Hydrogels for Aqueous Encapsulation and Controlled Release of Hydrophilic Model Drugs. *Biomacromolecules*. 2005;6(4):2131-2139. doi:10.1021/bm050116t
44. Greene MK, Johnston MC, Scott CJ. Nanomedicine in Pancreatic Cancer: Current Status and Future Opportunities for Overcoming Therapy Resistance. *Cancers*. 2021;13(24):6175. doi:10.3390/cancers13246175
45. Caputo D, Pozzi D, Farolfi T, Passa R, Coppola R, Caracciolo G. Nanotechnology and pancreatic cancer management: State of the art and further perspectives. *World J Gastrointest Oncol*. 2021;13(4):231-237. doi:10.4251/wjgo.v13.i4.231
46. Pazenir | European Medicines Agency. Accessed April 11, 2024. https://www.ema.europa.eu/en/medicines/human/EPAR/pazenir
47. About ABRAXANE® and Metastatic Pancreatic Cancer Overview. Accessed May 10, 2024. https://www.abraxane.com/mpac/abraxane-and-advanced-pancreatic-cancer
48. Research C for DE and. FDA approves irinotecan liposome for first-line treatment of metastatic pancreatic adenocarcinoma. *FDA*. Published online February 16, 2024. Accessed May 10, 2024. https://www.fda.gov/drugs/resources-information-approved-drugs/fda-approves-irinotecan-liposome-first-line-treatment-metastatic-pancreatic-adenocarcinoma
49. Leys C, Ley C, Klein O, Bernard P, Licata L. Detecting outliers: Do not use standard deviation around the mean, use absolute deviation around the median. *J Exp Soc Psychol*. 2013;49(4):764-766. doi:10.1016/j.jesp.2013.03.013
50. Danaei M, Dehghankhold M, Ataei S, et al. Impact of Particle Size and Polydispersity Index on the Clinical Applications of Lipidic Nanocarrier Systems. *Pharmaceutics*. 2018;10(2):57. doi:10.3390/pharmaceutics10020057
51. Kemp JA, Kwon YJ. Cancer nanotechnology: current status and perspectives. *Nano Converg*. 2021;8(1):34. doi:10.1186/s40580-021-00282-7